Iranian Journal of Geophysics, Vol 19 No 3, 2025, Page 1 – 23 (Research Article)
DOI: 10.30499/ijg.2024.441596.1573

Evaluation of crustal stress from estimation of b-value based on tectonic regions in the north part of the Zagros in Iran

Samira Musavian [1] and Mehrdad Mostafazadeh [2*]

[1] *Ph.D. Candidate, International Institute of Earthquake Engineering and Seismology, Tehran, Iran*
[2] *Assistant Professor in Seismology, International Institute of Earthquake Engineering and Seismology, Tehran, Iran*

(Received: 05 February 2024, Accepted: 03 April 2024)

Abstract

In this study, a high-resolution map of the Gutenberg–Richter b-value and differential stress field and stress drop contour map are provided for the north part of the Zagros region. This region is important because more than 10 earthquakes with magnitude greater than 6 occurred in this region in the last century. In order to understand the tectonic stress pattern of the region, the catalogue of seismicity between 1900 and 2020 was used (most of the events that could be used in this region) in order to explore the spatial and temporal variations of the b-value, which corresponds to the slope of the frequency-magnitude distribution of the earthquakes. The differential crustal stress from the b-value was estimated and focused on estimating the b-value first in the whole north of the Zagros belt and then in 3 sub-regions. For the entire north of Zagros and its sub-regions, the average content of M_c is 4.0 for the region that has catalogs with different Mc in the time domain and the content of b-value in this region is around 1.03 to 1.12 and the b-value is gradually have lower value, from west to the East of Zagros. In all earlier studies, the b-value was estimated for the entire Zagros but in this study, we estimated the b-value based on the tectonic units of the region. In a temporal variation of b-value, one minimum in the diagram of b-value in MFF region can be seen exactly before the 12 Nov. 2017 Ezgeleh earthquake (M_w=7.3) and another minimum in the diagram would be related to the 18 August 2014 Mormori earthquake (M_w=6.2).

The stress drop was estimated from M_0 for the north part of the Zagros and then this value was compared in the time period before and after the Ezgele earthquake. The stress drop value before and after the Ezgeleh earthquake, around the epicenter, was changed between 0.024-0.03 before the earthquake to 0.13-0.261 MPa after the earthquake respectively. Finally, the differential stress value is calculated in the time period before and after Ezgele Earthquake, around the epicenter, and it is changed between 300-322 MPa before the earthquake to 238-295 MPa after the earthquake respectively. Therefore, we infer that stress is transmitted from the northern part of the area to the central part of it.

Keywords: b-value, differential stress, Ezgele, north of Zagros, seismicity, stress drop

[*]Corresponding author: mehrdad@iiees.ac.ir

1 Introduction

Zagros belt is one of the youngest and one of the most active continental belts in the world (Stöcklin, 1974). Due to the convergence of Iran-Arabia (Fig. 1), the NW–SE-, Zagros Mountains are still under deformation with a convergence rate (22 ± 2 mm/y)(Vernant et al., 2004). The most of seismic activity with a magnitude greater than 6 (there are more than 10 events) occurred in the north part of the Zagros (see Table 1& Fig.1). The earthquakes in the Zagros are distributed across a ~ 200 km wide zone. Commonly across the master blind thrust faults (Berberian 1995), within the thick sedimentary layer between 8 and 14km beneath the Hormuz Salt Formation (Ni and Barazangi, 1986)and (Hessami, Koyi, Talbot, Tabasi, and Shabanian, 2001) no rupture is visible in the surface.

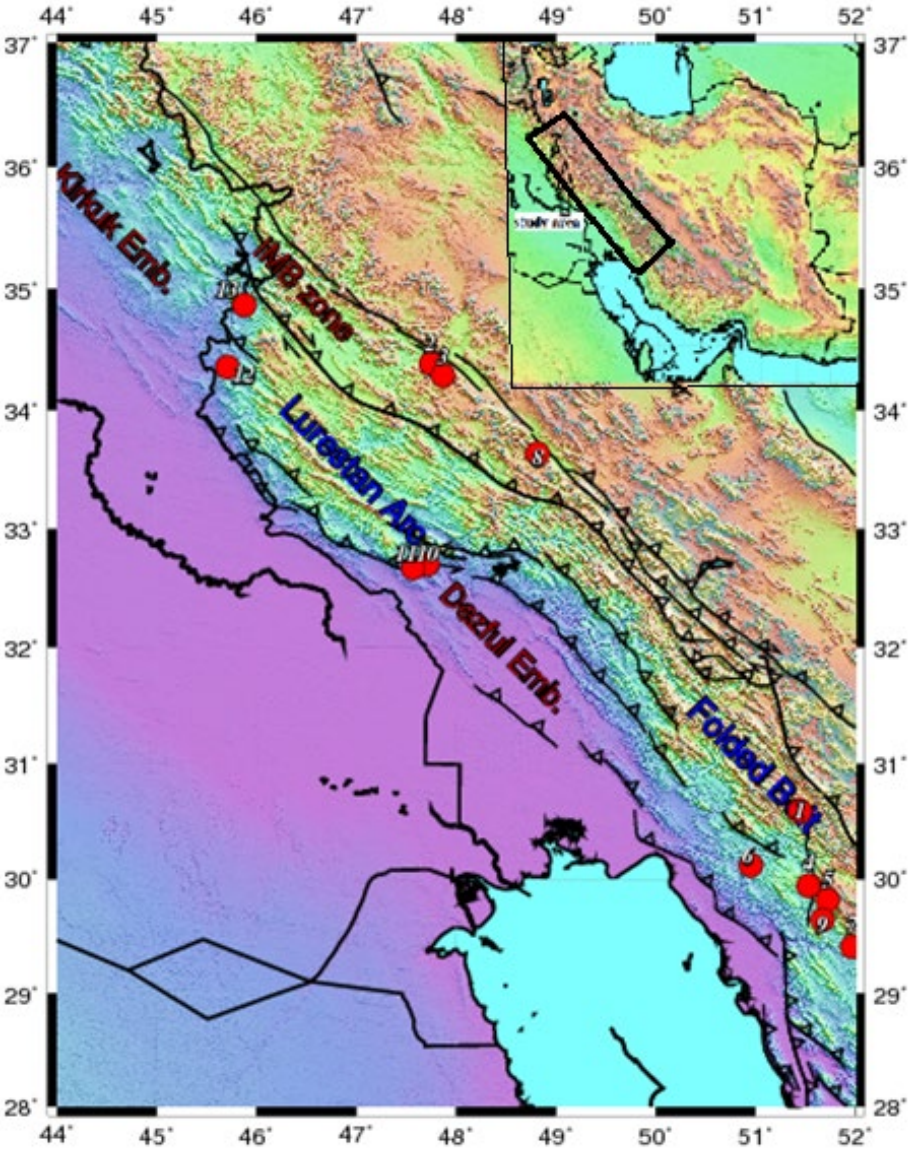

Figure1. Region of the study and location of 13 destructive events in the region based on table1.

Table1. Earthquakes with M_W greater than 6 in north part of Zagros belts from 1900 to 2020.

	Date	longitude	latitude	M_W	Depth	Time (hour& min)	Reference
1	1934-02-04	51.44	30.59	6.3	15	13:27	ISC
2	1957-12-12	41.74	34.38	6.4	15	01:45	ISC
3	1958-08-16	47.86	43.29	6.5	15	19:13	ISC
4	1986-07-12	51.53	29.94	6.1	12.1	07:54	ISC
5	1988-08-11	51.72	29.82	6.1	22.3	16:04	ISC
6	1989-05-27	50.95	30.12	6.1	10	20:08	ISC
7	1999-05-06	51.97	29.41	6.2	23.3	23:00	ISC
8	2006-03-31	48.81	33.63	6.1	15.7	01:17	ISC
9	2010-09-27	51.67	29.64	6.2	25	11:22	ISC
10	2014-08-18	47.71	32.70	6.2	12.9	02:32	ISC
11	2014-08-18	47.57	32.67	6.1	15.7	11:51	ISC
12	2017-11-12	45.88	34.87	7.3	20.1	21:48	ISC
13	2018-11-25	45.71	34.36	6.4	10.5	08:31	ISC

The b-value which is the slope of the frequency-magnitude distribution as introduced by (Gutenberg & Richter, 1944): $\log N = a - b*M$, where N is the cumulative number of seismic events of magnitude greater than or equal to M and a is related to the number of events. This equation shows the more frequent occurrence of small earthquakes compared to great earthquakes. The b-value is close to unity in most of the regions; a small b-value shows a deficit of small events or an excess of large events with respect to the mean relationship. Most of the studies of regional or global seismicity have explored the possible relationships between the b-value and some geophysical or geological parameters such as volcanic activity, crustal heterogeneity, earthquake phenomena, and so on. Finally, all these cases mostly outline spatial and temporal crustal stress variations (Ahmadzadeh, Parolai, Javan-Doloei, & Oth, 2017; Bachmann, Wiemer, Goertz-Allmann, & Woessner, 2012; El-Isa & Eaton, 2014; Görgün, 2013; Tal & Hager, 2015). It is also observed that the b-value is negatively correlated with the crustal differential stress ($\sigma1-\sigma3$), b-value decreases with increasing differential stress (El-Isa & Eaton, 2014; C. H. Scholz, 2015; Spada, Tormann, Wiemer, & Enescu, 2013). Moreover, the b-value decreases with depth to a minimum value (maximum differential stress), which mostly located in the region of the rupture initiation of the major earthquake

Also, a sudden decrease of the b-value is sometimes found before the occurrence of main shocks in large earthquakes (El-Isa & Eaton, 2014; Görgün, 2013; Zhang & Zhou, 2016) and a low b-value near active faults is most of the time interpreted as future asperities (Tormann, Wiemer, & Mignan, 2014). Then, a low b-value may be of an expressive increased probability of a major earthquake occurrence in the near future. This may be of interest in

regions of moderate seismic activity where large earthquakes often occur, as in the northern part of Zagros (such as the Ezgele earthquake, 2017). We propose here to quantify the b-value in the Northern part of Zagros, first of all, and then focusing on its variation in different Seismotectonic regions. The stress was also estimated (1) by computing the differential stress from the b-value using the relationship proposed by Scholz (2015) and (2) by estimating the stress drop from the magnitude and computing a especial formula for stress drop in this region. The whole North of the Zagros is considered first of all; and secondly, the region is divided into 3 sub-regions according to Seismotectonics (Berberian, 1995; Vergés et al., 2011). Exploring the b-values and crustal stresses (differential stress and Stress drop) with their possible correlations, this paper's goal is to explore the properties of the North Zagros crust and its mechanical behavior.

Additionally, in this paper, this idea is reviewed that the Gutenberg-Richter b-value may qualitatively be used as a stress scale (Bachmann et al., 2012) and thus reflects valuable information about the present-day Seismotectonics of North Zagros region and also, regions with low b-values are used to interpreted as future asperities (Tormann et al., 2014).

Therefore, the goal of this study is to obtain a high-resolution map of the b-value using the most unified and homogeneous part of the seismicity record of the region (from 1900 to July 2020). The correlations between seismic stress drop, b-value variations, and differential stress are also explored. This can help in providing important constraints when analyzing the state of present-day crustal stress within the region.

2 North Zagros context

The Zagros Mountains are the result of the Arabia/Eurasia collision which started at about 35 Ma when the rifted Arabian lithosphere was underthrusted beneath the Iranian plateau. The crustal thickening of it started about 12-25Ma (Early Miocene stage) (Mouthereau, Lacombe, & Vergés, 2012).

The Zagros belts are defined as NW–SE trading which has 2000 Km length from east Anatolian fault from eastern Turkey to the Makran subduction zone in southern Iran and its elevations are maximum near Khuzestan (Mouthereau et al., 2012)

GPS velocities show present-day convergence rate of Arabia and Eurasia is 19-23 mm/year which 7-10 mm of it, absorbed in Zagros (Hessami, Nilforoushan, & Talbot, 2006; Vernant et al., 2004).

The Zagros Mountains (Fig. 2) consist of three main Tectonic region including, southwest to northeast, the Persian Gulf Basin, the Zagros Fold-Thrust Belt (ZFTB), and the Zagros Imbricated Zone (IMBZ). The ZFTB, as the external part of the Zagros Mountains, includes three sub regions: the Zagros Fore deep Zone, the Mountains Front Flexure Zone (MFF), and the Simply Folded Belt (SFB) (Alavi, 2007; Berberian, 1995). In this region, there are three Seismotectonic formations, namely the Kirkuk Embayment, the Lurestan Arc, the Dezful Embayment (Fig.2) (Alavi, 2007; Stöcklin, 1968). This regions and sub regions of the north Zagros are mainly separated by the master blind thrust faults (Fig. 2), such as the Main Front Fault (MFF), the High Zagros Fault (HZF), the Main Recent Fault (MRF), and the Main Zagros Thrust Fault (MZT), as introduced by (Berberian, 1995; Vergés et al., 2011). For this study, the north Zagros region is divided into 3 sub tectonic regions (simply folded belts [SFB], Mountain front fault [MFF], and Imbricated zone [IMBZ]), and boundary regions in the North part of the Zagros are used (Vergés et al., 2011). Most of the current shortening is being accumulated at MFF (Mouthereau et al., 2012).

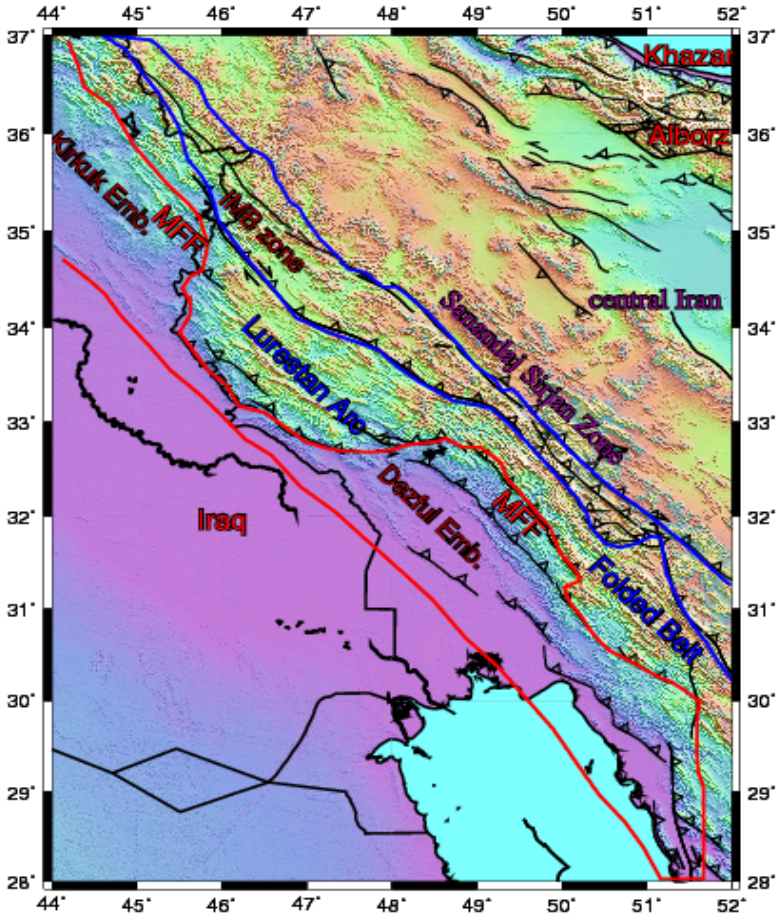

Figure2. Different tectonic zones in north part of Zagros belts. As you can see, we have tree main zones in this part of Zagros (Imbricated zone, MFF zone and simply folded belts) and some formation like (Dezful Emb. Lurestan Arc and Sanandaj-Sirjan zone) (Berberian. 1995 and Verges. 2011).

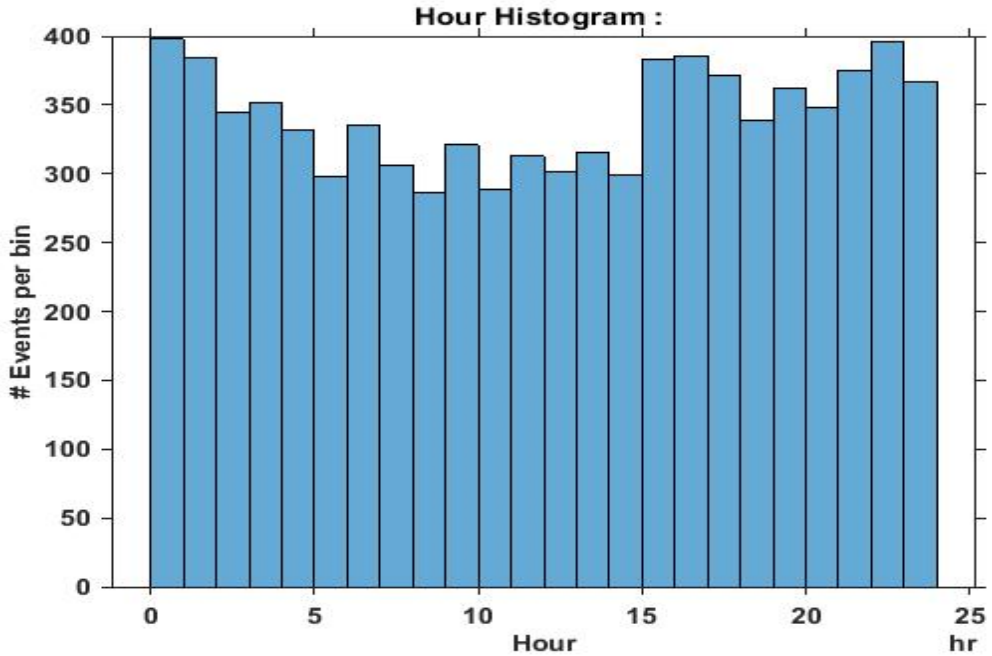

Figure3. Number of events for hours of the day in the North Zagros data set during 1900-2020. As you can see, there is not any difference between numbers of events in day and night.

These basement-involved thrust faults cut through the folded sedimentary layer and control the deformation of the cover in a thin-skinned tectonic regime (Berberian, 1995). The Zagros accommodates extreme, low- to moderate-magnitude seismic events (Barnhart, Lohman, & Mellors, 2013). The lower Cambrian Hormuz, consisting of salt formation units and shales in the Lurestan Arc, detach the sedimentary cover from the crystalline basement (Alavi, 2007; Berberian, 1995; McQuarrie, 2004). Thus, due to the influence of the Hormuz formations, surface faulting in the Zagros is observed in uncommon options (Talebian & Jackson, 2004; Walker et al., 2005). The surface is truncated and accommodates parallel folds (Nissen, Tatar, Jackson, & Allen, 2011) .Deformation in the Zagros is also accommodated along some transverse faults (Fathian et al., 2021). These deep-seated, basement-involved Pan-African structures have repeatedly displaced fold axes, and seismicity patterns (Fig. 2). Lateral displacement of the MFF (Fig. 2) is also a result of the reaction of these strike-slip faults (Hessami et al., 2001) bounding Lurestan (Alavi, 2007). (Hessami et al., 2001), suggested that some strike-slip faults are associated with a few moderate to large magnitude earthquakes signifying these faults, are aseismic and it seems that deformation along them occurs as creeping.

3 Data and methods

3.1 Zagros seismicity

A seismicity catalog for the region was compiled (44◦E − 52◦E and 29◦N − 37◦N) using one international (the Intereismological Center (IRSC)) (IRSC; http://irsc.ut.ac.ir/bulletin.php) databases for the time period of January 1900 to July 2020. The M_N magnitude modified version (Rezapour, 2005) is the dominant magnitude scale reported by the IRSC catalog of the University of Tehran, while, mb, M_W, M_L, and M_S are the major magnitude scales provided for reported events by ISC. The conversion relations between these magnitude scales have been suggested for the region (Ahmadzadeh et al., 2017; KADİRİOĞLU & Kartal, 2016; Mousavi-Bafrouei, Mirzaei, & Shabani, 2014; Shahvar, Zare, & Castellaro, 2013). To avoid differences in magnitude scales, we simply considered magnitude scales of events with M < = 5 to be equal to moment magnitude M_w (Heaton & Kanamori, 1984). For events, the unified catalog consists of 4,373 events in the northern part of the Zagros in this study, the orthogonal regression relations proposed by (Mousavi-Bafrouei et al., 2014) are used to convert different magnitude scales in each database to the moment magnitude M_w. Therefore, the magnitude scale of all events in this data set is conversed to Mw with the following relations (Mousavi-Bafrouei et al., 2014):

A) m_b to M_w:

$$Mw = 1.207(\pm0.039)\, mb - 0.933(\pm0.193), \quad (1)$$

$R2 = 0.73$, $\nu = 0.24$, $n = 353$, $3.9 \leq mb \leq 6.1$, $h = 0.22$

B) M_s to M_w:

$$Mw = 0.679(\pm0.017)\, Ms + 2.004(\pm0.075), \quad (2)$$

$R2 = 0.88$, $\nu = 0.16$, $n = 407$, $3 \leq Ms \leq 6.1$, $h = 0.12$

The original catalogue of events (from 1990 to 2020) has been declustered by the method proposed by (Reasenberg, 1985). In this study, first, the entire catalogue is considered and then the catalog is divided into three Seismotectonic zones including Mountain Front Fault (MFF), simply folded belts (SFB), and Imbricated zone (Berberian, 1995; Vergés et al., 2011) as depicted Fig. 2.

Figure 3 shows the number of events that occurred during the day for the original catalog of the Zagros. Ambient noise during daytime hours causes a decrease in the number of detected events during daytime hours. The numbers of events during daytime hours are not more

than the number of events during the night. Therefore, the original catalog of the Zagros, which is used here, is not contaminated by mine explosion (Gulia, Wiemer, & Wyss, 2010).

3.2 Methodology

3.2.1 b-value

The b-value is the slope of frequency–magnitude distribution (FMD) (Gutenberg and Richter.1944):

$$\log_{10}N=a-bM \quad (3)$$

Where N is the number of events with magnitude greater than or equal to M and '**a**' is a constant. The b value is usually estimated by the least squares method. The b value is obtained from a complete catalog that contains events with a magnitude larger or equal to Mc of the catalog (Wyss, Sammis, Nadeau, & Wiemer, 2004). Equation (3) is applicable to a homogeneous catalog with constant Mc during time (Wyss et al., 2004).

In the data set of the north Zagros zone, there are three main sub-catalogs with different Mc in time intervals 1964–1998 and 1990–2018 (Fig. 4). (Kijko & Sellevoll, 1989) introduced a method, based on maximum likelihood estimation, to calculate the b value of a seismic catalog with time intervals of different Mc. Using a catalog containing 's' sub catalogs with different Mc, the likelihood function of seismicity parameters for the whole of the catalog is defined as (Kijko & Sellevoll, 1989):

$$L(\theta|X)=\prod_{i=0}^{s}L_i(\theta|X_i) \quad (4)$$

Where L (θ|X) is the likelihood function of seismicity parameters of the ith sub catalog, X_i is the magnitude of earthquakes of the ith sub catalog, seismicity parameters θ= (β,λ); λ is the earthquake activity rate, β is related to b value as b = β log e, and 'e' is the Neperian number. If the magnitude of earthquakes is independent of earthquakes number, the likelihood function of seismicity parameters θ of ith sub catalog can be written as the product of likelihood functions of parameters β and λ, then, Eq. (4) can be written as:

$$L(\theta|X)=\prod_{i=0}^{s}L_{i\beta}.L_{i\lambda} \quad (5)$$

Using the maximum likelihood method, estimating parameter β is accompaniedby putting the first derivation of the likelihood function in terms of parameter β equal to zero:

$$\partial \ln L(\theta|X)/\partial\beta=0 \quad (6)$$

In this study, because the values of M_c are variable in time, Kiko's method is used to estimate the b-value (Kijko & Sellevoll, 1989).

The b-value displays the ratio of the number of smaller to larger earthquakes (Gutenberg & Richter, 1944). Higher b values have been observed in areas where smaller earthquakes are more frequent than larger ones, whereas lower b-values are estimated in areas where larger earthquakes are more frequently occurred. The b-value variations may therefore have an important role in improving our physical understanding and forecasting earthquakes (Herrmann, Piegari, & Marzocchi, 2022).

3.3 Differential stress

Considering the seismicity analysis by (Spada et al, 2013) for magnitudes greater than 2.5 in various continental domains and for different styles of deformation, Scholz (2015) defined a relationship between b-value and differential stress ($\sigma_1-\sigma_3$) as follows:

$$b = 1.23 \pm 0.06 - (0.0012 \pm 0.0003)\,(\sigma_1 - \sigma_3), \quad (7)$$

Where ($\sigma_1-\sigma_3$) is in mega Pascal. The author shows that this relationship explains that both the seismicity distribution with depth and the type of focal mechanism are related to the b-value.

This equation outlines the negative correlation between the two variables, a high b-value corresponds to a low differential stress, and a low b-value to a high differential stress.

It is necessary to notice that, in relation (7), if the b-value is greater than 1.23, (σ1–σ3) is negative, which is unmeaning in

physics. It must be kept in mind that relation (7) results from the linear fit of a large number of scattered data where some b-values exceed 1.23. It is thus a simplified model. This marks the limits of the use of this relation as values of b greater than 1.23 are not fine.

3.4 Stress drop

Having no approach to waveforms, we cannot calculate the stress drop through the spectral analysis of the P- and S-waves. So we can estimate the stress drop to evaluate the corner frequency and the radius of the seismic sources. This analysis was done by (Mostafazadeh & Mokhtari, 2003) of magnitude ranging from 4 to 7.5. These data were used to establish a relation between the seismic source radius r and the seismic moment Mo (Fig 4).

We obtained the following power law as providing a reasonably good fit of the data with a coefficient of correlation of 50% (Fig 5):

$$r = 0.5362 M_0^{0.2395} \quad (8)$$

Where M_0 is in Newton meter and r (source radius) in meter. Then, the stress drop is obtained with the empirical relation (Eshelby, 1957; Madariaga, 1979)

$$\sigma = \frac{7M0}{16r^3} \quad (9)$$

Where M_0 is in newton per meter, **r** in meters, and $\Delta\sigma$ in Pascal (Mega Pascal). Combining equations (8) and (9) gives:

$$\Delta\sigma = 2.838\ Mo^{0.2815} \quad (10)$$

M_0 is deduced from the magnitude by the relation (Hanks & Kanamori, 1979)

$$M_w = 2/3 \log M_0 - 6.01 \quad (11)$$

Equation (10) can be an estimate of stress drop based on $\mathbf{M_0}$ for North Zagros. Of course, the determinations of the source radius **r** and of the stress drop $\mathbf{\Delta\sigma}$ are less rigorous here than by using the spectral method as proposed by Ahmadzadeh et al (2017).

4 Uncertainties

Uncertainties on the b-value are determined in ZMAP by a bootstrap approach. We obtain b-value uncertainties varying between 0.04 and 0.09 with a mean value of 0.07. Then, it was considered that b-values with uncertainties greater than 0.15 are unstable and they are not taken into account in our results, discussion, and interpretati

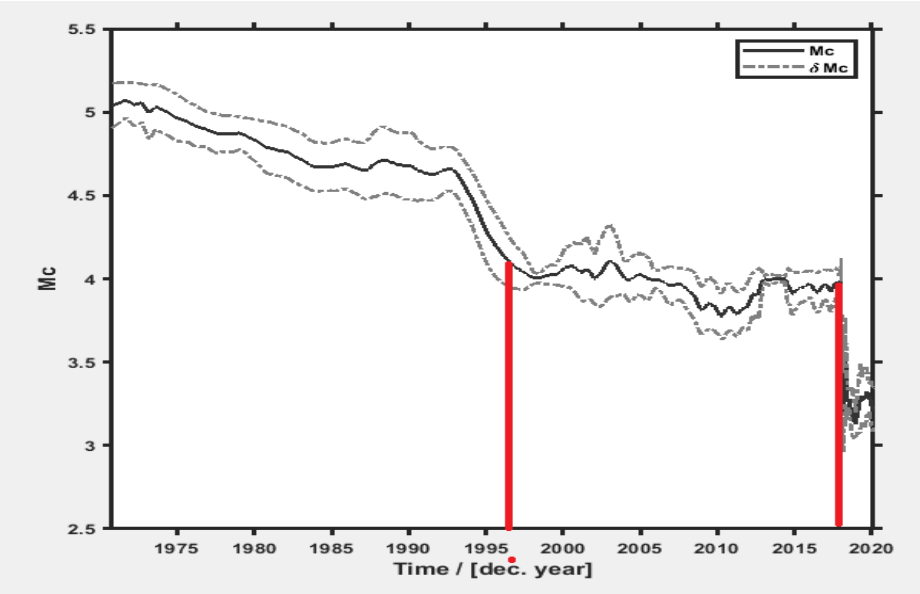

Figure 4. Variations and maximum value of completeness magnitude (*Mc*) during 1900-2020 in original curvature method catalog of the North Zagros. The completeness magnitudes are estimated using maximum (Wiemer and Wyss 2000) and moving window approach with a window of 200 events by 150 events. Dashed lines indicate one standard deviation from the average. The uncertainties in the completeness magnitudes (dashed lines) are obtained from *N* =200 bootstrap samples. Average of Mc in this figure is 4.3.

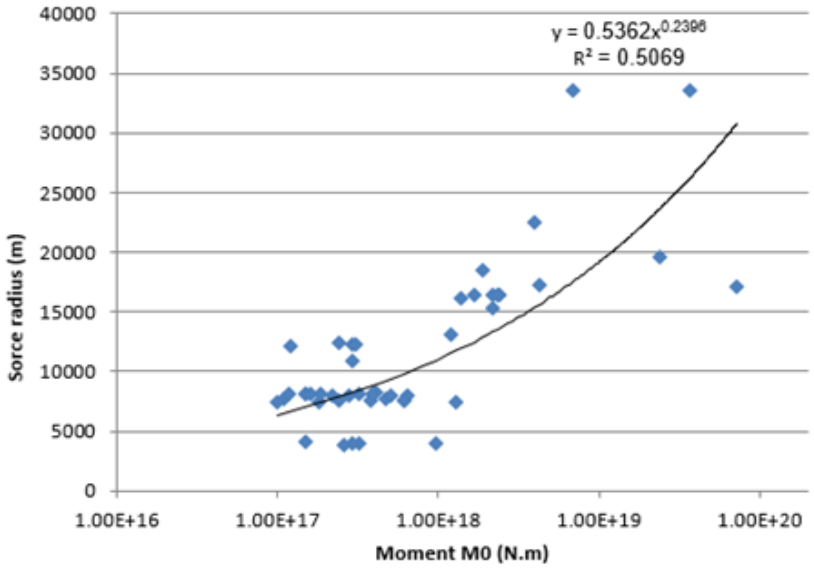

Figure 5. Power law relationship between the seismic source radius, r, and the scalar moment, Mo, determined from previous Zagros seismic parameters published before (Mostafazadeh and Mokhtari, 2003).

5 Results

5.1 The whole catalogue

The original catalogue of events (from 1990 to 2020) has been declustered by the method proposed by (Reasenberg, 1985). The magnitude of completeness (Mc) was first determined for the entire catalogue of the north Zagros seismicity at 4.0 ± 0.2 with the (Kijko & Sellevoll, 1989) method for the catalogs that have different M_c in the time domain (Fig.6, Table 2). Then, the events with a magnitude smaller than 4.0 were removed from the catalogue, reducing the number of events from 4373 to 1367 for which we obtained b = 1.06 ± 0.03 (Table 2).

The b-value for the whole catalogue was compared, in the time period of 1900 – 2020. It can be seen in (Fig6, right), a minimum near 2014, and after that the b-value increases until 2018 and decreases again.

In this period, we have two important earthquakes; Mormori (2014) and Ezgele (2017) (Fig 11). M_w for both of these earthquakes is greater than 6 which was incredible in this region.

Also the b-value can be estimated on the surface for all north of the Zagros (Fig .7). As you know, areas that have lower b-value, in the young Seismotectonic with high seismicity such as Zagros, are the stress accumulated area (locked segments). In Fig (7), the north part of the study area; there is an area with a lower b-value so it can be considered as a possible place for future earthquakes.

5.2 Regional variations

In order to have more detail about the b-value and stress relationship, all the above process for sub-regions of north Zagros was calculated based on the regions that (Berberian, 1995; Vergés et al., 2011) were introduced for Zagros tectonics. According to their study, the North part of the Zagros is divided into three Seismotectonic zones (Fig2& Table 2). The b-values with the number of events used in each zone and the magnitude of completeness, Mc, for each zone and also the b-value chart in the time domain were determined. Then the b-value in two dimensions was calculated and illustrated (table 2 &Fig 4 to 11).

Table 2. Magnitude of completeness (M_c), b-value, number of events (N) and number of events with magnitude greater than or equal to M_c (N_c) for the complete catalogue of seismicity (All), for three tectonic zones of north Zagros.

Zone	M_c	b-value	N/Nc
North Zagros	4.0±0.2	1.04±0.03	4373/1367
1. MFF	4. 0±0.2	1.19±0.04	1825/567
2. SFB	4.0 ±0.2	1.03±0.07	2108/493
3. IMBZ	4.0±0.2	0.98±0.1	426/85

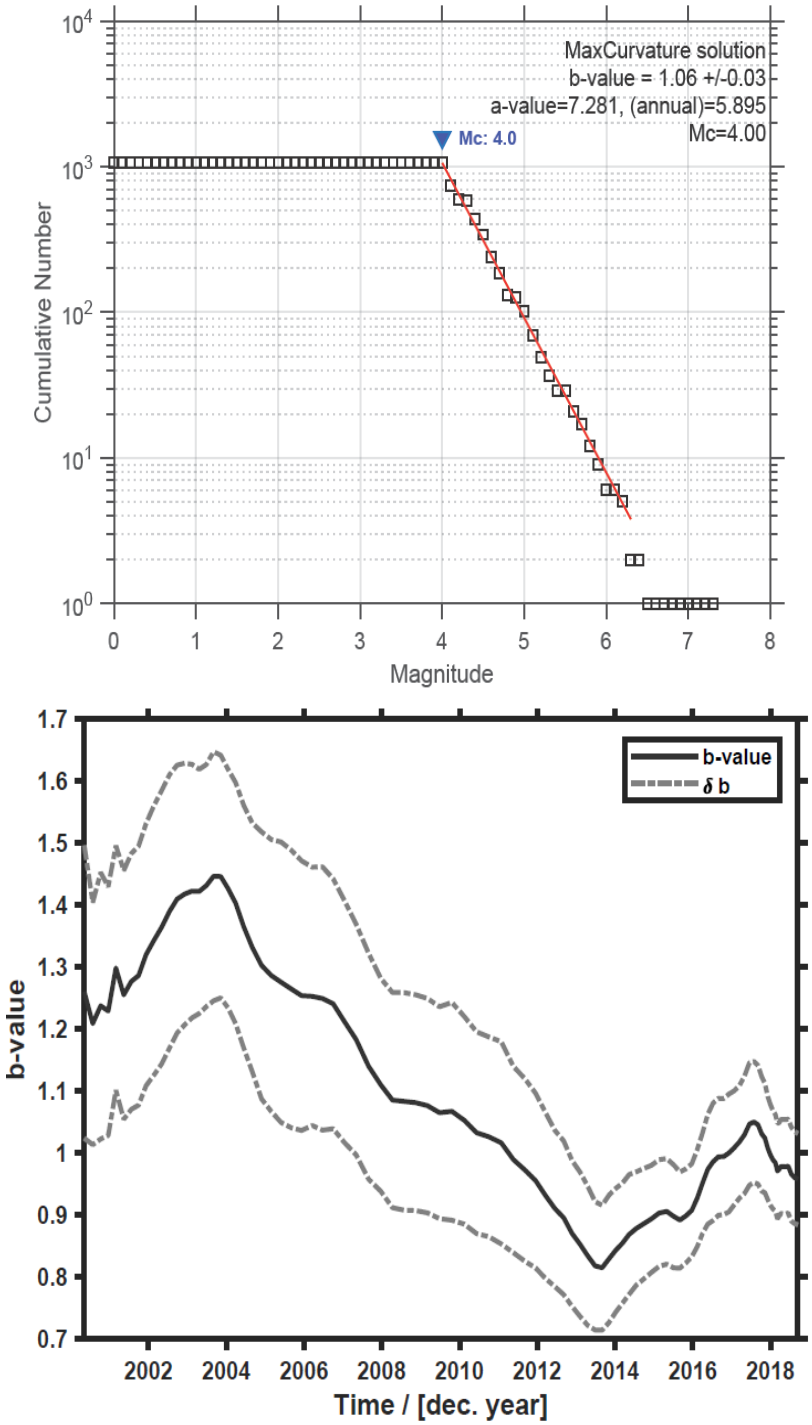

Figure 6. Magnitude of completeness Mc and b-value for time interval 1900–2020 by using maximum likelihood method for the north of Zagros catalog (left). B-value in time domain in north Zagros catalog (right).

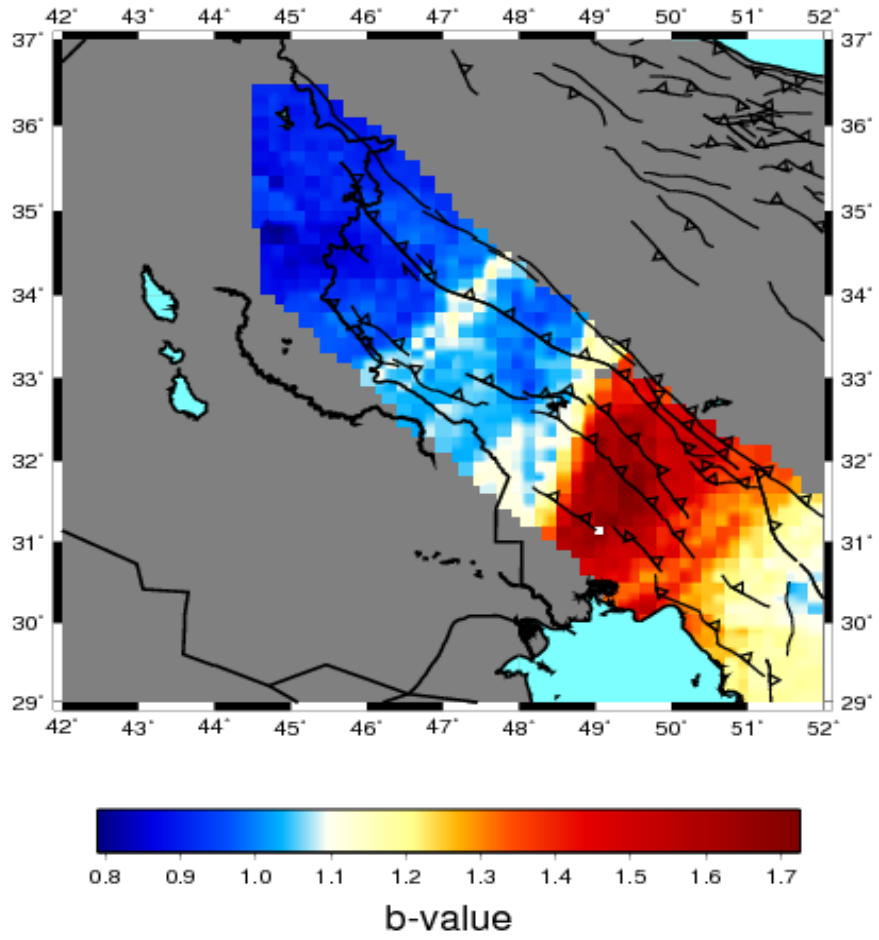

Figure 7. Spatialvariation of b-value for north Zagros catalog in time period of 1900-2020.

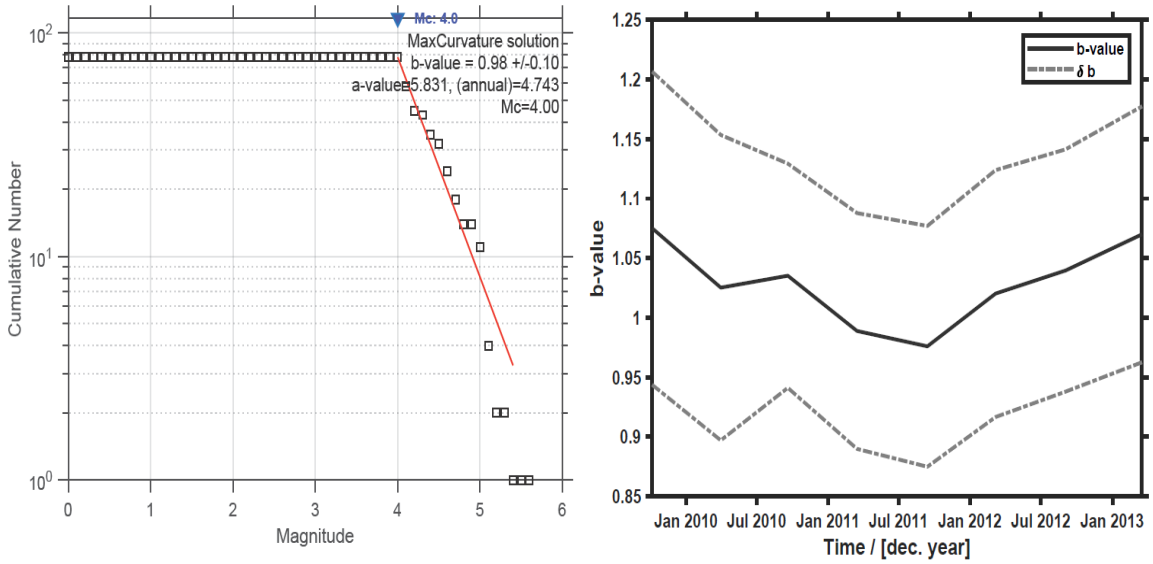

Figure 8. Magnitude of completeness Mc and b-value for time interval 1900–2020 by using maximum likelihood method for the IMB zone catalog (left). B-value in time domain in IMB (right).

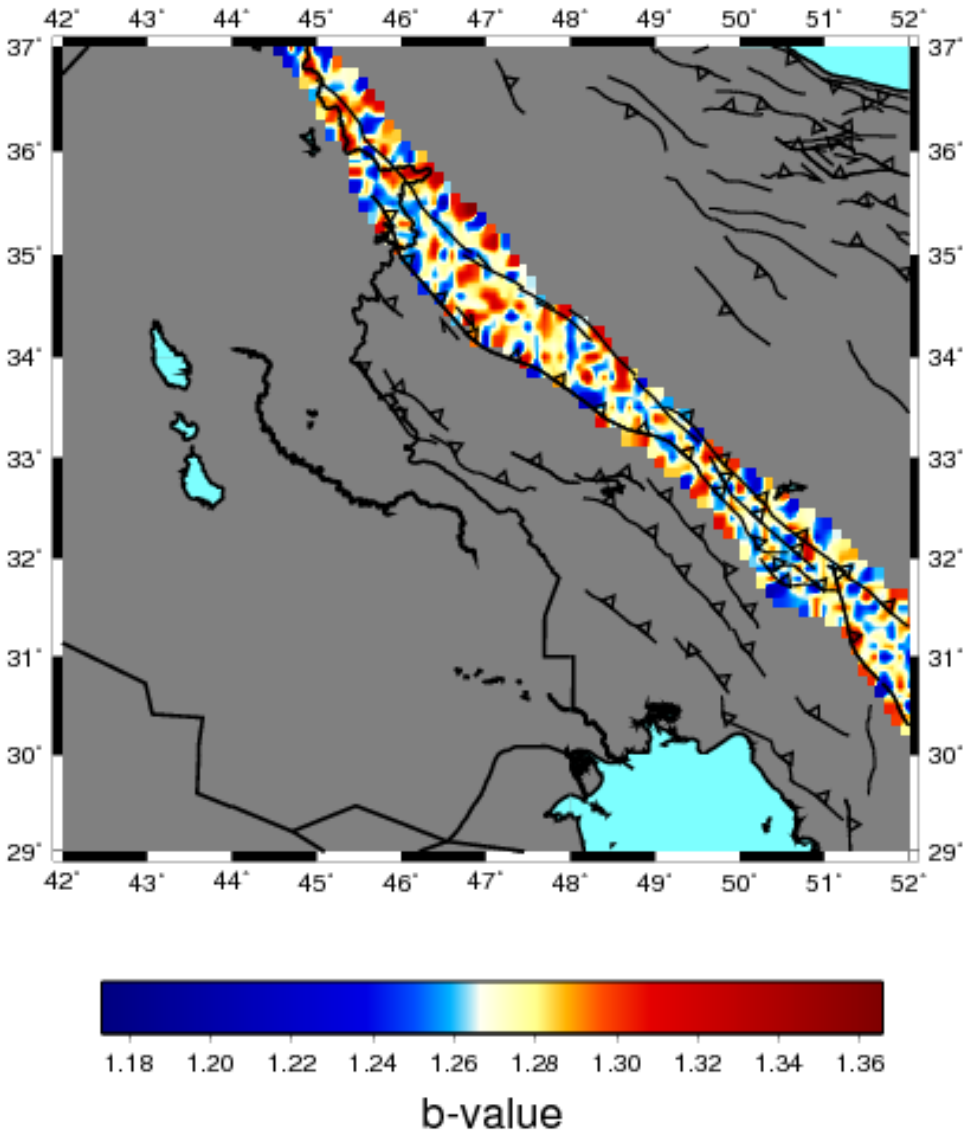

Figure 9. Spatial variation of b-value for IMB zone catalog in time period of 1900-2020.

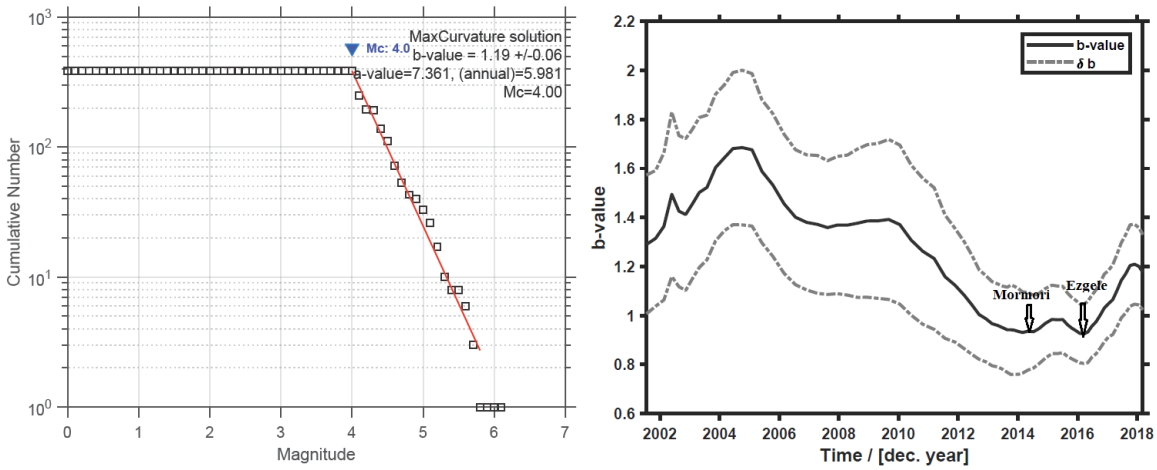

Figure 10. Magnitude of completeness Mc and b-value for time interval 1900–2020 by using maximum likelihood method for MFF, you can see two minimum before Mormori and before Ezgele earthquak.

1-For Imbricated zone (IMBZ); M_c was determined equal to 4.0±0.2 and so b-value would be 0.98±0.09. For the b-value chart in the time domain, near 2014, it had the lowestcontent shown in Fig.8. After that in Fig .9 it can be seen b-value in two dimensions in this region.

2-In the Mountain Front Fault (MFF) zone, the Mc is 4.0±0.2 and the b-value and the Ezgele 2017 earthquake both of them was happened in the MFF zone. Then at last one can be seen the b-value in surface in Figure 11.

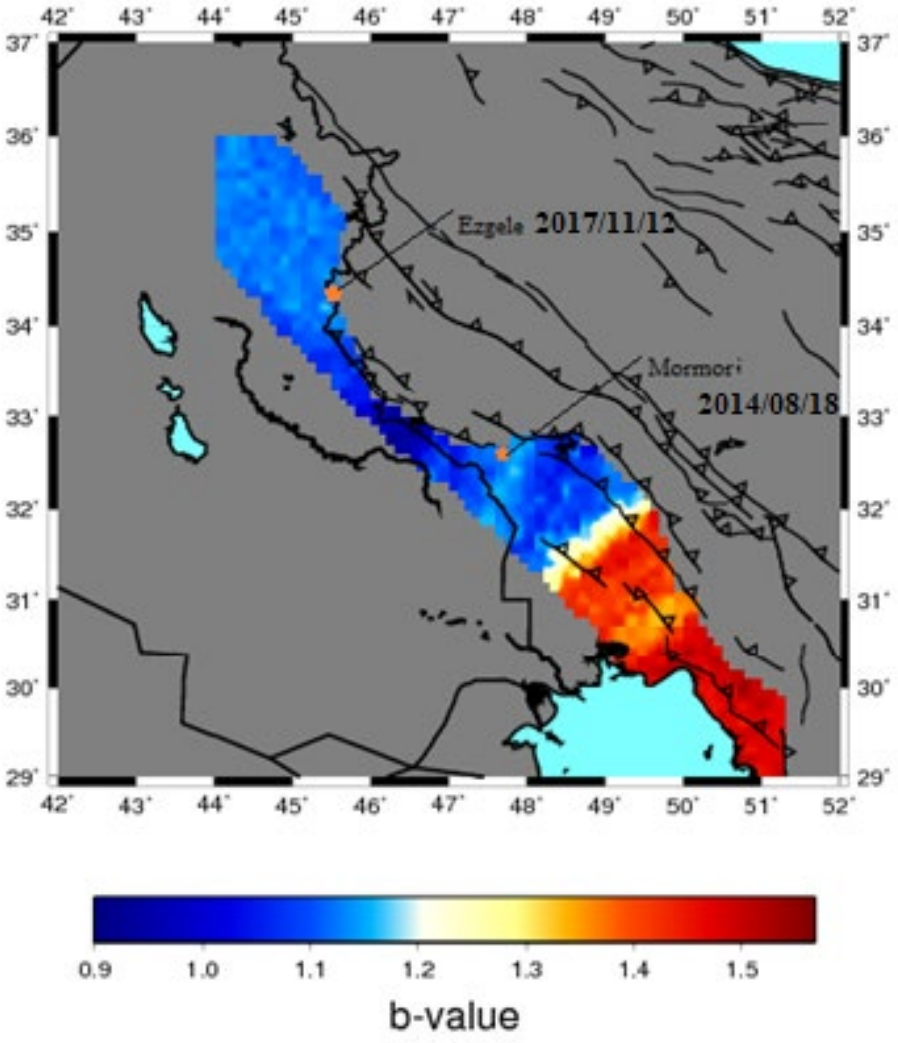

Figure 11. Spatial variation of b-value forMFF zone, you can see the location of Ezgele (2017/11/12) and Mormori (2014/08/18) earthquakes in this figure.

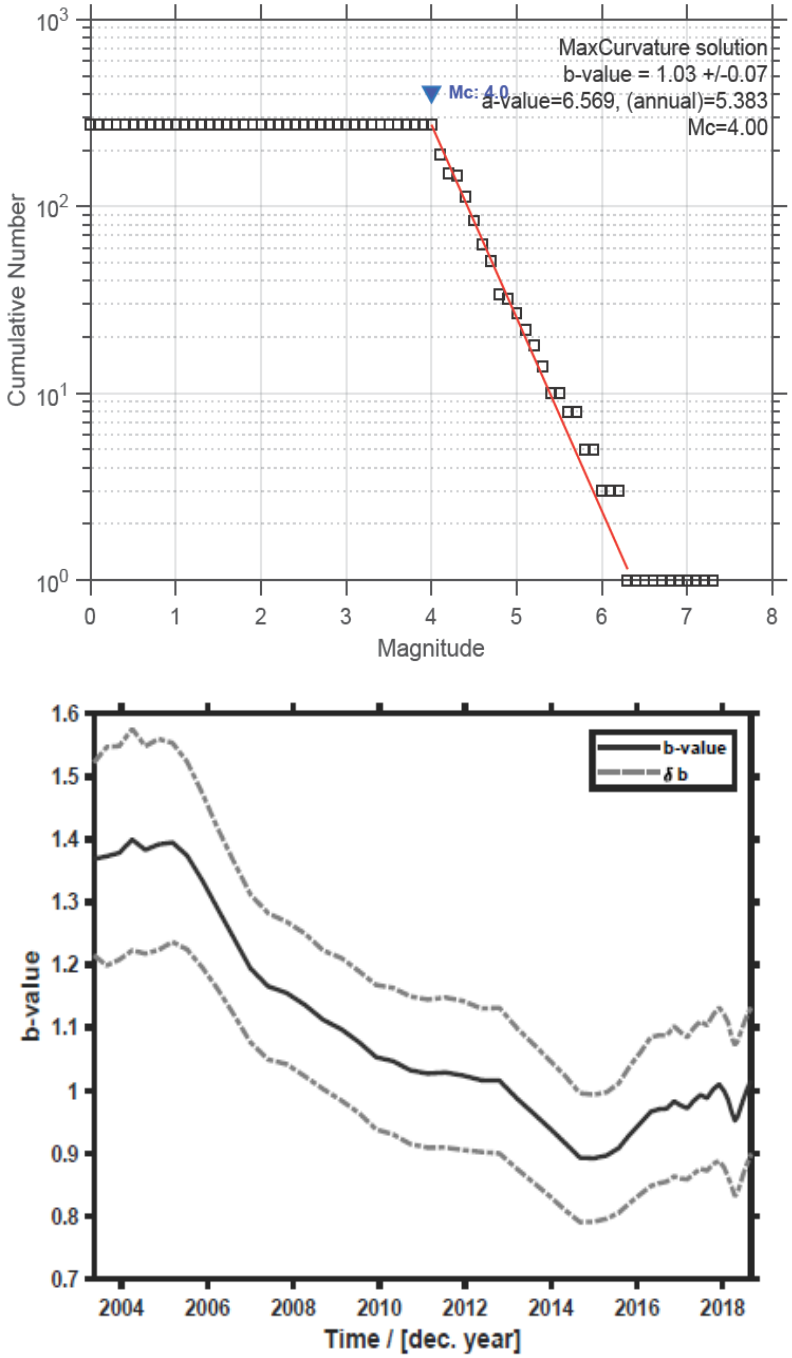

Figure 12. Magnitude of completeness Mc and b-value for time interval 1900–2020 by using maximum likelihood method for the SFB zone.

3-The last zone is simply folded belt (SFB); Mc for SFB again is 4.0±0.2 and b-value would be 1.03±0.07. For the b-value chart in the time domain, one minimum in b-value near 2015 can be seen in Fig.12, and the b-value in the surface was shown in Fig.13.

In the following, the b-value was calculated for the same time (3 years) before and after the Ezgele earthquake (2017) and then the b-value before and after the Ezgele earthquake was drowned in two dimensions in Fig.14. As it can be seen in Fig.14, the value of b, around Ezgele earthquake that before earthquake has lower value (b-value was less than 1) than after the earthquake (b-value is more than1).

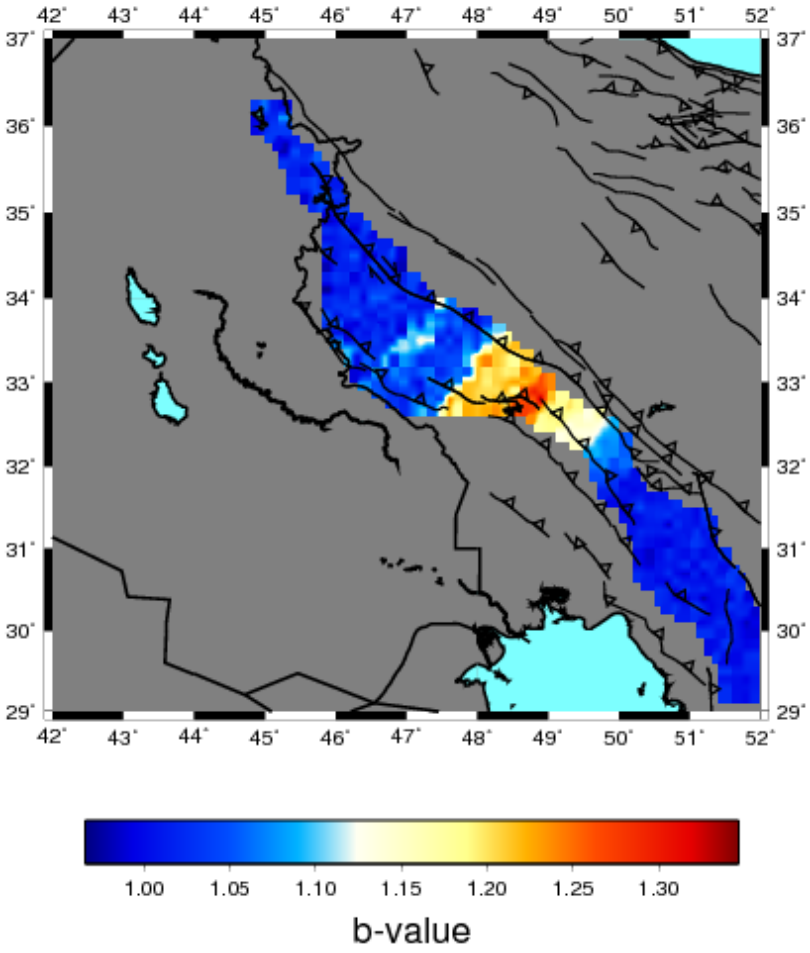

Figure13. Spatial variation of b-value forSFB zone catalog (left). B-value in time domain in SFB (right).

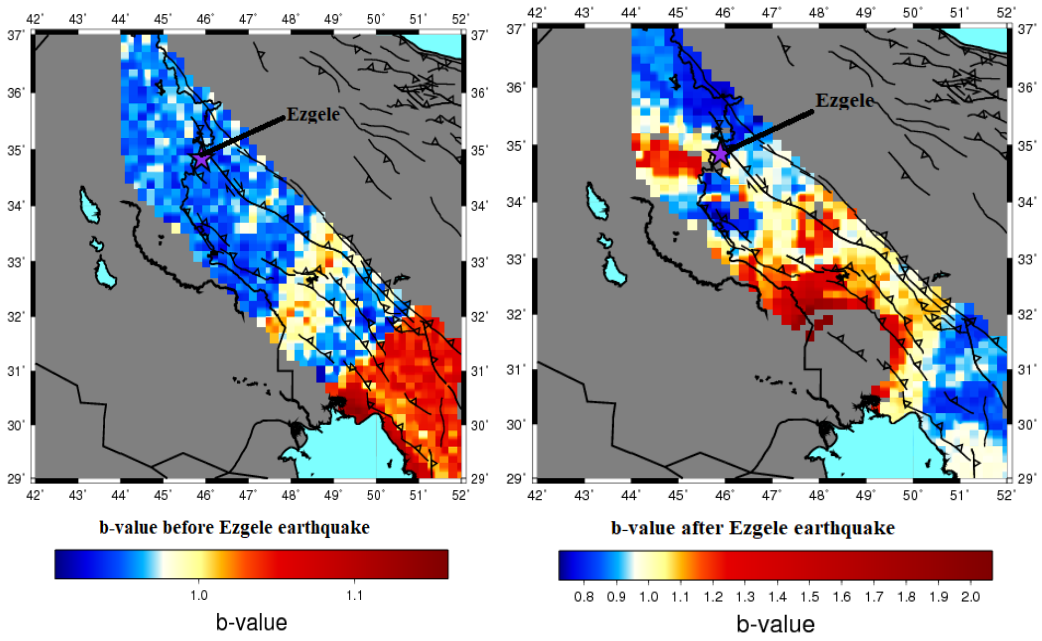

Figure 14. Variations of b-value in the surface before Ezgele earthquake.

For the last part of the study, the stress drop estimation and differential stress (σ1–σ3) were demonstrated in the contour map, which is linearly negatively correlated with b, Fig.15, Fig. .16., Fig.17 and Fig.18. Also the particular formula for stress drop in the north of Zagros (equation 10) was determined.

In the final part of this study, the differential stress and stress drop before and after the Ezgele earthquake in November of 2017 in the entire north of the Zagros belts was illustrated. The amount of Differential stress was 300-322 MPa before the earthquake and 283-295 MPa after the earthquake (Figs.15 and 16). For stress drop before and after Ezgele 2017 earthquake, it was between 0.024 - 0.03 MPa. But after the earthquake, the value of stress drop is between 0.13 - 0.26 Mpa.

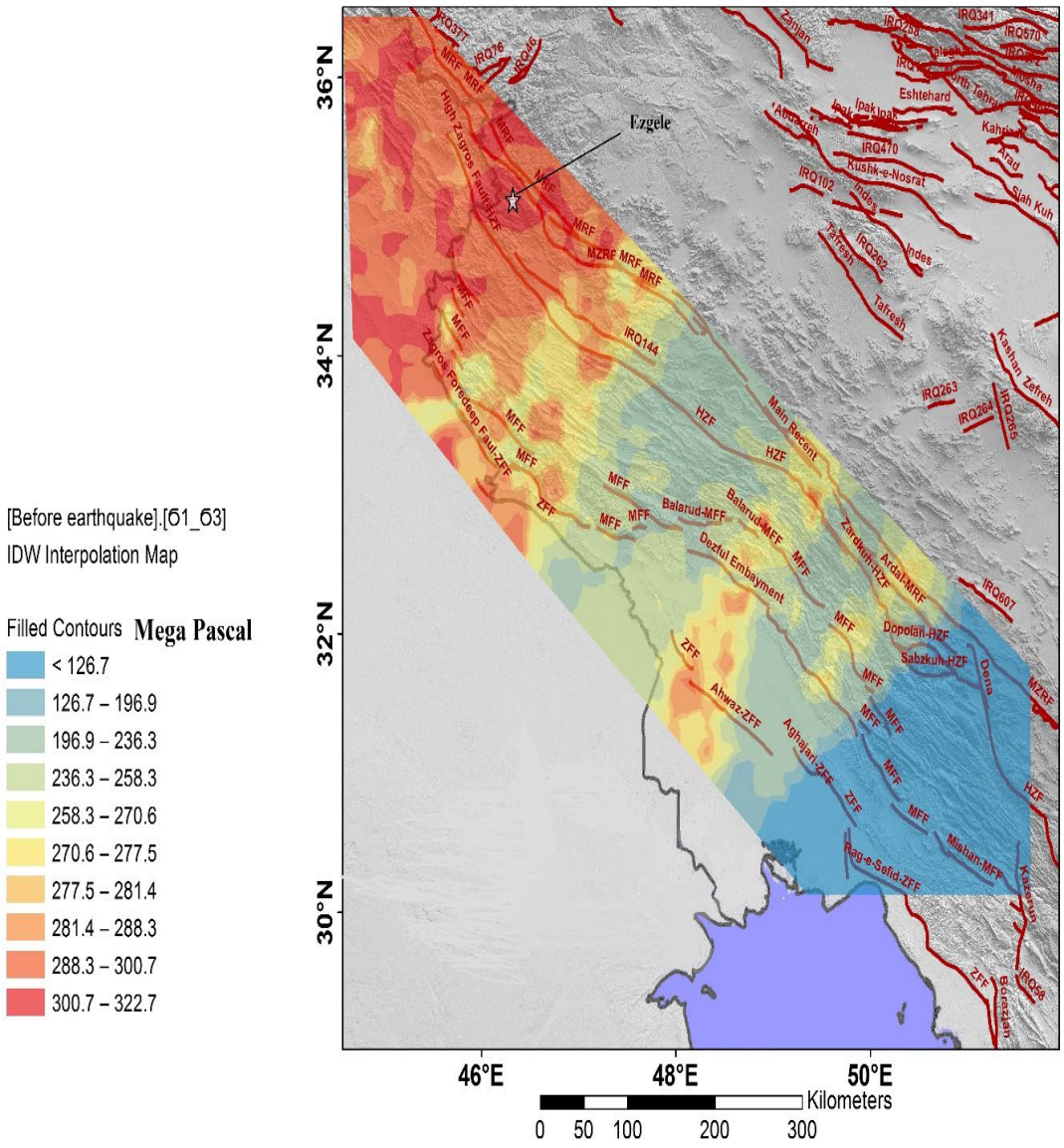

Figure 15. Contour map of differential stress field (б1-б3) estimates the diagram in two dimension before Ezgeleh 2017 earthquake. As you can see, differential stress in Ezgele and around, had high value of stress in mega Pascal.

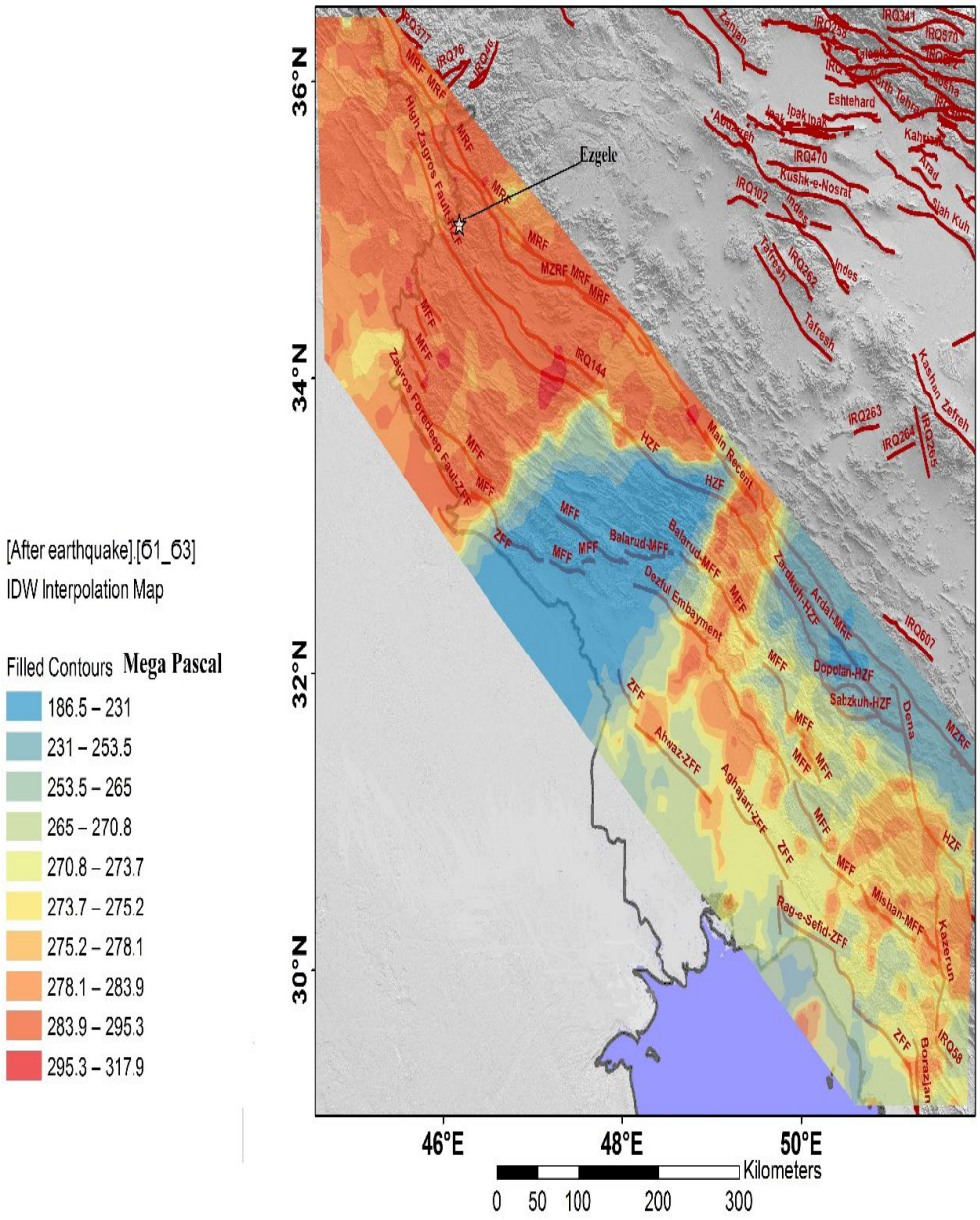

Figure 16. Contour map of differential stress field (б1-б3) estimates the diagram in two dimension after Ezgeleh 2017 earthquake. As you can see, differential stress in Ezgele and around, had lower value of stress than before Ezgele earthquake.

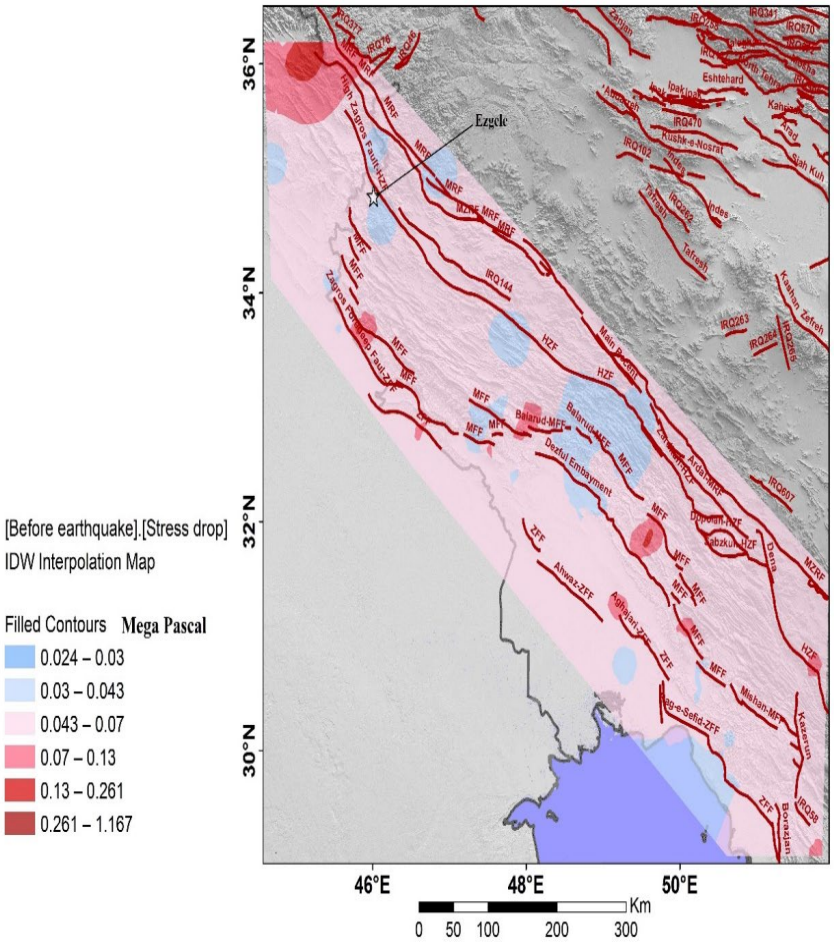

Figure 17. Contour map of Stress drop in north part of the Zagros before Ezgele earthquake.

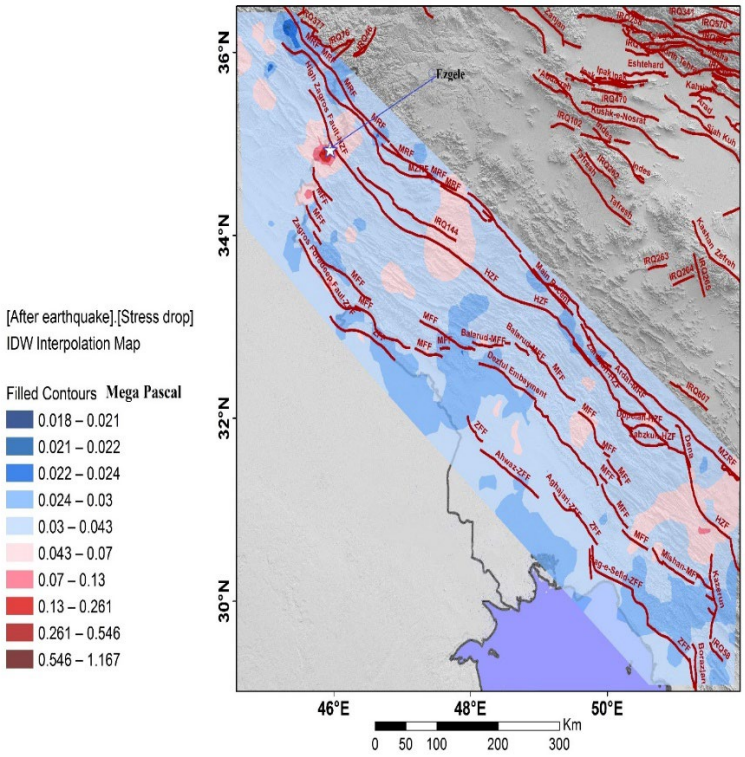

Figure 18. Contour map of Stress drop in north part of the Zagros after Ezgele earthquake. As you can see in Figure 17 and Figure 18.

6 Discussion and conclusion

The north part of the Zagros is characterized by an orogenic-scale deformation partitioning (Berberian, 1995; Vergés et al., 2011) with a belt-parallel right-lateral slip along the Main Recent Fault (MRF) (Tchalenko & Braud, 1974) and a belt-perpendicular shortening across the Zagros Simple Folded Belts (SFB), which are separated by the crushed zone of the High Zagros Belt (HZB) along the High Zagros Fault.

The average b-value in previous articles is close to the constant 1.0 (Frohlich & Davis, 1993), b-values in the range of 1-1.2 have been reported for tectonic events. Also, different parameters can cause this variation. One of these parameters that its influence on the b-value has been shown in laboratory and field experiments, is the stress condition. Many studies have reported an inverse relation between stress and the seismic b-value (C. Scholz, 1968; C. H. Scholz, 2015; Wiemer & Wyss, 1997). On the other hand, direct relationships have been observed between the b-value and thermal gradient (Bachmann et al., 2012; Warren & Latham, 1970) pore pressure (Bachmann et al., 2012), and material heterogeneity (Mogi, 1962)Moreover, effects of some other parameters such as faulting styles (Nakaya, 2005, 2006), earthquake size (Hamilton & McCloskey, 1997), earthquake depth (Wiemer & Wyss, 1997), and Geotectonical characteristics (Niazi, 1984) on the seismic b-value have been investigated.

(Mousavi-Bafrouei et al., 2014) estimated average b-values for the five Seismogenic zones of the Alborz-Azerbaijan, central-east Iran, Kopeh-Dagh, Makran, and Zagros for three time periods of 1900–1963, 1964–1996, and 1997–2012. (Mousavi, 2017) with declusterd catalog estimated the same results as was estimated here for North Zagros. (Madahizadeh, Mostafazadeh, & Ashkpour-Motlagh, 2016) have also reached similar results in different parts of Zagros. Although agreements among the results of our study and previous studies for different time periods might suggest the existence of a general permanent pattern in this region, however, the observed strong b-value anomalies (for instance within the northern and southern North Zagros) indicate that a more detailed spatial mapping might be preferable. Therefore, to estimate the b-value as a forecasting factor in large earthquakes, it is better to use more accurate methods which has a tectonic base. As it can be seen in this study, in the chart of the b-value in time domain, in North Zagros, for the complete catalog, a clear minimum before the Ezgale 2017 earthquake was not observed (see Fig.6). But after dividing the catalog, based on the tectonics of the region, in the MFF region, in b- value chart in the time domain, two clear minima can be seen, which are related to two big earthquakes of Murmuri and Azgeleh Kermanshah in this tectonic zone (Fig.10). As a result, according to the chart of b-value in the time domain, the occurrence of such earthquakes in this region is not an unusual phenomenon.

This research also is emphasized on Ezgele (2017) earthquake which occurred on (2017/11/12) with a moment magnitude (Mw=7.3) in the MFF zone. This earthquake was the greatest earthquake which was happened in Zagros in the last century and most of the building in Ezgele and Sarpol-e Zahab was destroyed completely.

For more details, the entire catalog of north Zagros was used and in almost the same time period before the Ezgele earthquake and after it, the b-value for each sub region was estimated and also drew the b-value diagram in the surface and compared together (Fig14). It seems the b-value had a lower value around the epicenter in the time period before the main shock. Also from west to east of the north part of the Zagros (MFF to IMBZ),

the b-value has a lower value (Table 2). It means that seismicity decreases moving from MFF to IMBZ. So, we expected lower seismicity and earthquake with higher $M_{w.}$

With the relationship of b-value and differential stress (equation.7), The differential stress (Ϭ1-Ϭ3) was determined and then the contour map of it in two dimensions (Fig15 and Fig16) was drawn. As can be seen in Fig (15 and Fig16), (Ϭ1-Ϭ3) had higher values before the Ezgele earthquake. After the earthquake, it shows lower values. It is clear in Fig 15 and 16 that, there is stress transmittal from the north part of Zagros to the central part of it.

At last, for the stress drop, was estimated in the same time period before and after the Ezgele earthquake about 3 years as discussed in section 3.4. Then the diagrams of the contour map of stress drop were plotted in two dimensions (Figs.17 and 18). As can be observed in (Figs.17 and 18), completely different values of stress drop before and after Ezgele 2017 are illustrated. It can be seen in Fig.18, that the stress drop value before and after the earthquake, around the epicenter was changed between 0.024-0.03 for the time before the earthquake to 0.13-0.261 MPa after the earthquake.

The seismicity analysis described in this paper helped us understanding the stress state related to different episodes of deformation distributed across the belt under an oblique plate convergence. These results suggested that the stress has coincided with the transition from thin- to thick-skinned collision.

Acknowledgements

The authors sincerely thank Dr.Yasamin Izadkhah who edited this article. We also thank Dr.Movaghari and Ms.Mahshadnia who helped us draw figures and also we thank the International Institute of Earthquake Engineering and Seismology (IIEES) and the Iranian Seismological Center (IRSC) we used their catalog for this project. This work was supported by the International Institute of Earthquake Engineering and Seismology (iiees) unde project [792-5411]).

References

Ahmadzadeh, S., Parolai, S., Javan-Doloei, G., & Oth, A. (2017). Attenuation characteristics, source parameters and site effects from inversion of S waves of the March 31, 2006 Silakhor aftershocks. Annals of geophysics, 60(Suppl. to 6).

Alavi, M. (2007). Structures of the Zagros fold-thrust belt in Iran. American Journal of science, 307(9), 1064-1095.

Bachmann, C. E., Wiemer, S., Goertz-Allmann, B., & Woessner, J. (2012). Influence of pore-pressure on the event-size distribution of induced earthquakes. Geophysical research letters, 39(9).

Barnhart, W. D., Lohman, R. B., & Mellors, R. J. (2013). Active accommodation of plate convergence in Southern Iran: Earthquake locations, triggered aseismic slip, and regional strain rates. Journal of Geophysical Research: Solid Earth, 118(10), 5699-5711.

Berberian, M. (1995). Master "blind" thrust faults hidden under the Zagros folds: active basement tectonics and surface morphotectonics. Tectonophysics, 241(3-4), 193-224.

El-Isa, Z. H., & Eaton, D. W. (2014). Spatiotemporal variations in the b-value of earthquake magnitude–frequency distributions: Classification and causes. Tectonophysics, 615, 1-11.

Eshelby, J. D. (1957). The determination of the elastic field of an ellipsoidal inclusion, and related problems. Proceedings of the royal society of London. Series A. Mathematical and physical sciences, 241(1226), 376-396.

Fathian, A., Atzori, S., Nazari, H., Reicherter, K., Salvi, S., Svigkas, N., .

. . Yaminifard, F. (2021). Complex co- and postseismic faulting of the 2017–2018 seismic sequence in western Iran revealed by InSAR and seismic data. Remote Sensing of Environment, 253, 112224.

Frohlich, C., & Davis, S. D. (1993). Teleseismic b values; or, much ado about 1.0. Journal of Geophysical Research: Solid Earth, 98(B1), 631-644.

Görgün, E. (2013). Analysis of the b-values before and after the 23 October 2011 Mw 7.2 Van–Erciş, Turkey earthquake. Tectonophysics, 603, 213-221.

Gulia, L., Wiemer, S., & Wyss, M. (2010). Theme IV–Understanding Seismicity Catalogs and Their Problems Catalog artifacts and quality control. In CORSSA: the Community Online Resource for Statistical Seismicity Analysis (pp. 1-26): CORSSA: the Community Online Resource for Statistical Seismicity Analysis.

Gutenberg, B., & Richter, C. F. (1944). Frequency of earthquakes in California. Bulletin of the Seismological Society of America, 34(4), 185-188.

Hamilton, T., & McCloskey, J. (1997). Breakdown in power-law scaling in an analogue model of earthquake rupture and stick-slip. Geophysical research letters, 24(4), 465-468.

Hanks, T. C., & Kanamori, H. (1979). A moment magnitude scale. Journal of Geophysical Research: Solid Earth, 84(B5), 2348-2350.

Heaton, T. H., & Kanamori, H. (1984). Seismic potential associated with subduction in the northwestern United States. Bulletin of the Seismological Society of America, 74(3), 933-941.

Herrmann, M., Piegari, E., & Marzocchi, W. (2022). Revealing the spatiotemporal complexity of the magnitude distribution and b-value during an earthquake sequence. Nature Communications, 13(1), 5087.

Hessami, K., Koyi, H. A., Talbot, C. J., Tabasi, H., & Shabanian, E. (2001). Progressive unconformities within an evolving foreland fold–thrust belt, Zagros Mountains. Journal of the Geological Society, 158(6), 969-981.

Hessami, K., Nilforoushan, F., & Talbot, C. J. (2006). Active deformation within the Zagros Mountains deduced from GPS measurements. Journal of the Geological Society, 163(1), 143-148.

KADİRİOĞLU, F. T., & Kartal, R. F. (2016). The new empirical magnitude conversion relations using an improved earthquake catalogue for Turkey and its near vicinity (1900-2012). Turkish Journal of Earth Sciences, 25(4), 300-310.

Kijko, A., & Sellevoll, M. A. (1989). Estimation of earthquake hazard parameters from incomplete data files. Part I. Utilization of extreme and complete catalogs with different threshold magnitudes. Bulletin of the Seismological Society of America, 79(3), 645-654.

Madahizadeh, R., Mostafazadeh, M., & Ashkpour-Motlagh, S. (2016). Earthquake Potential in the Zagros Region, Iran. Acta Geophysica, 64, 1462-1494.

Madariaga, R. (1979). On the relation between seismic moment and stress drop in the presence of stress and strength heterogeneity. Journal of Geophysical Research: Solid Earth, 84(B5), 2243-2250.

McQuarrie, N. (2004). Crustal scale geometry of the Zagros fold–thrust belt, Iran. Journal of structural Geology, 26(3), 519-535.

Mogi, K. (1962). Magnitude-frequency relation for elastic shocks accompanying fractures of various materials and some related problems in earthquakes. Bull. Earthq. Res. Inst., Univ. Tokyo, 40, 831-853.

Mostafazadeh, M., & Mokhtari, M. (2003). Source Time Function of Caspian Basin and Surrounding Area Earthquakes. Journal of Seismology and Earthquake Engineering, 5(3), 17-26.

Mousavi-Bafrouei, S. H., Mirzaei, N., & Shabani, E. (2014). A declustered earthquake catalog for the Iranian Plateau. Annals of geophysics, 57(6).

Mousavi, S. M. (2017). Mapping seismic moment and b-value within the continental-collision orogenic-belt region of the Iranian Plateau. Journal of Geodynamics, 103, 26-41.

Mouthereau, F., Lacombe, O., & Vergés, J. (2012). Building the Zagros collisional orogen: timing, strain distribution and the dynamics of Arabia/Eurasia plate convergence. Tectonophysics, 532, 27-60.

Nakaya, S. (2005). Fractal properties of seismicity in regions affected by large, shallow earthquakes in western Japan: Implications for fault formation processes based on a binary fractal fracture network model. Journal of Geophysical Research: Solid Earth, 110(B1).

Nakaya, S. (2006). Spatiotemporal variation in b value within the subducting slab prior to the 2003 Tokachi-oki earthquake (M 8.0), Japan. Journal of Geophysical Research: Solid Earth, 111(B3).

Ni, J., & Barazangi, M. (1986). Seismotectonics of the Zagros continental collision zone and a comparison with the Himalayas. Journal of Geophysical Research: Solid Earth, 91(B8), 8205-8218.

Niazi, M. (1984). Regression analysis of reported earthquake precursors. I. Presentation of data. pure and applied geophysics, 122, 966-981.

Nissen, E., Tatar, M., Jackson, J. A., & Allen, M. B. (2011). New views on earthquake faulting in the Zagros fold-and-thrust belt of Iran. Geophysical Journal International, 186(3), 928-944.

Reasenberg, P. (1985). Second-order moment of central California seismicity, 1969–1982. Journal of Geophysical Research: Solid Earth, 90(B7), 5479-5495.

Rezapour, M. (2005). Magnitude scale in the Tabriz seismic network. J Earth Space Phys, 31(1), 13-21.

Scholz, C. (1968). The frequency-magnitude relation of microfracturing in rock and its relation to earthquakes. Bulletin of the Seismological Society of America, 58(1), 399-415.

Scholz, C. H. (2015). On the stress dependence of the earthquake b value. Geophysical research letters, 42(5), 1399-1402.

Shahvar, M. P., Zare, M., & Castellaro, S. (2013). A unified seismic catalog for the Iranian plateau (1900–2011). Seismological Research Letters, 84(2), 233-249.

Spada, M., Tormann, T., Wiemer, S., & Enescu, B. (2013). Generic dependence of the frequency-size distribution of earthquakes on depth and its relation to the strength profile of the crust. Geophysical research letters, 40(4), 709-714.

Stöcklin, J. (1968). Structural history and tectonics of Iran: a review. AAPG bulletin, 52(7), 1229-1258.

Stöcklin, J. (1974). Possible ancient continental margins in Iran. In The geology of continental margins (pp. 873-887): Springer.

Tal, Y., & Hager, B. H. (2015). An empirical study of the distribution of earthquakes with respect to rock type and depth. Geophysical research letters, 42(18), 7406-7413.

Talebian, M., & Jackson, J. (2004). A reappraisal of earthquake focal mechanisms and active shortening in the Zagros mountains of Iran. Geophysical Journal International, 156(3), 506-526.

Tchalenko, J., & Braud, J. (1974). Seismicity and structure of the Zagros (Iran): the Main Recent Fault between 33 and 35 N. Philosophical Transactions of the Royal Society of London. Series A, Mathematical and Physical Sciences, 277(1262), 1-25.

Tormann, T., Wiemer, S., & Mignan, A. (2014). Systematic survey of high-resolution b value imaging along Californian faults: Inference on asperities. Journal of Geophysical Research: Solid Earth, 119(3), 2029-2054.

Vergés, J., Goodarzi, M., Emami, H., Karpuz, R., Efstathiou, J., & Gillespie, P. (2011). Multiple detachment folding in Pusht-e Kuh arc, Zagros: Role of mechanical stratigraphy.

Vernant, P., Nilforoushan, F., Hatzfeld, D., Abbassi, M., Vigny, C., Masson, F., . . . Bayer, R. (2004). Present-day crustal deformation and plate kinematics in the Middle East constrained by GPS measurements in Iran and northern Oman. Geophysical Journal International, 157(1), 381-398.

Walker, R. T., Andalibi, M., Gheitanchi, M., Jackson, J., Karegar, S., & Priestley, K. (2005). Seismological and field observations from the 1990 November 6 Furg (Hormozgan) earthquake: a rare case of surface rupture in the Zagros mountains of Iran. Geophysical Journal International, 163(2), 567-579.

Warren, N. W., & Latham, G. V. (1970). An experimental study of thermally induced microfracturing and its relation to volcanic seismicity. Journal of Geophysical Research, 75(23), 4455-4464.

Wiemer, S., & Wyss, M. (1997). Mapping the frequency-magnitude distribution in asperities: An improved technique to calculate recurrence times? Journal of

Geophysical Research: Solid Earth, 102(B7), 15115-15128.

Wyss, M., Sammis, C. G., Nadeau, R. M., & Wiemer, S. (2004). Fractal dimension and b-value on creeping and locked patches of the San Andreas fault near Parkfield, California. Bulletin of the Seismological Society of America, 94(2), 410-421.

Zhang, S., & Zhou, S. (2016). Spatial and temporal variation of b-values in south-west China. pure and applied geophys-ics, 173, 85-96.